THE ASTROPHYSICAL JOURNAL, 268:185–194, 1983 May 1

SURVEY OF Hα EMISSION IN GLOBULAR CLUSTER RED GIANTS

C. CACCIARI[1]
ESTEC Astronomy Division, Villafranca, Spain

AND

K. C. FREEMAN
Mount Stromlo and Siding Spring Observatories, Research School of Physical Sciences,
The Australian National University

Received 1982 July 29; accepted 1982 October 22

ABSTRACT

From a spectroscopic survey (resolution 0.67 Å) of 143 red giants in 12 globular clusters and three open clusters, direct evidence of Hα emission was found for about one-third of the stars brighter than $\log (L/L_\odot) = 2.9$. There is no clear dependence of Hα emission (or mass loss rate) on metallicity. A few stars were observed many times over an interval of about 1 year, and there is clear evidence that the Hα emission is variable. From the distribution of stars in the $\log H_0$–M_{bol} plane (H_0 is the corrected FWHM for the apparent Hα absorption feature), we suggest that weak Hα emission (i.e., a lower rate of mass loss) may be present in most globular cluster giants with $\log (L/L_\odot)$ between 2.9 and 2.3 and perhaps even fainter. We argue that this Hα emission is associated with the main part of the pre–horizontal-branch mass loss.

Subject headings: clusters: globular — stars: emission-line — stars: late-type — stars: mass loss

I. INTRODUCTION

One of the theoretical requirements to account for the horizontal-branch (HB) morphology of globular clusters is a mass loss of a few tenths of a solar mass during the evolution preceeding the HB phase (Castellani and Renzini 1968; Iben and Rood 1970; Rood 1973). Similar conclusions were obtained earlier by Christy (1965, 1966) from his computations of RR Lyrae pulsation. Fusi Pecci and Renzini (1975, 1976) and Renzini (1977) discussed the possible mechanisms responsible for this mass loss and proposed an accoustically driven stellar wind model. Their theoretical formula gives a mass loss rate of the same order as the empirical formula proposed by Reimers (1975) for Population I red giants and fulfills the requirements for a total mass loss of about 0.2 $M_\odot$ on the red giant branch (RGB) and 0.1 $M_\odot$ on the asymptotic giant branch (AGB). According to this model, the stars at the tip of the RGB are expected to lose mass at a rate of a few times 10^{-8} $M_\odot$ yr^{-1}, and the expanding envelope thus formed could be detected by its Hα emission.

Cohen (1976, 1978, 1979, 1980, 1981), Mallia and Pagel (1978), and Peterson (1981, 1982) have reported the presence of weak emission components of Hα in the spectra of some of the brightest red giants in several globular clusters and also in the metal-poor field red giants HDE 232078 and HD 165195.

In this paper we present an extensive Hα spectroscopic survey of red giants in 12 globular clusters, covering a wide range of abundance, and also in three old open clusters. Mass loss rates are derived on the same assumptions used by Cohen (1976), and the observations are compared with the theoretical predictions of Fusi Pecci and Renzini's (1975) stellar wind model and with Reimer's (1975) semiempirical model. Evidence is presented that the emission components in the Hα profile are variable. Finally, the relation between the stellar luminosity and the FWHM of the Hα absorption feature is discussed.

[1] On leave from the Osservatorio Astronomico, Bologna, Italy.

II. OBSERVATIONS

The spectra were obtained between 1978 July and 1979 July at the coudé spectrograph of the 1.88 m telescope at Mount Stromlo Observatory. The dispersion was 14 Å mm^{-1}, the projected slit width was 45 μm or 0.63 Å, and the detector was the Photon Counting Array (PCA); this is an intensified Reticon array with photon event centering to half a diode, or 12 μm. The modulation transfer function is flat to a spatial frequency of 35 line pairs mm^{-1}. The PCA was used in the two-channel mode: star and sky were observed simultaneously. The spectra have about 500 photon counts per continuum channel (300 for some of the faintest stars), so the photometric accuracy is about 5% per channel (each channel is 12 μm or 0.17 Å) or about 2.5% per resolution element. The sky contribution was subtracted from the star spectrum, and the spectra were then smoothed by convolution with a Gaussian profile with a FWHM of 2.5 channels. The final smoothed instrumental profile has a FWHM of 4.0 channels or 0.67 Å.

In Table 1 we list the clusters observed and give the values of reddening, distance modulus, and metal abundance which will be used in § III*a* to derive the stellar parameters. The globular cluster abundances are from Zinn (1980), and the other parameters are from the references given in the footnotes to Table 1. The stars

TABLE 1

INTEGRATED PARAMETERS FOR CLUSTERS

Cluster	E_{B-V}	$(m-M)$	[Fe/H]	References
47 Tuc	0.04	13.5	−0.64	1, 2, 3
NGC 362	0.05	14.90	−1.13	4, 5, 6, 7
NGC 3201	0.21	14.20	−1.40	8, 9
ω Cen	0.11	13.92	−1.60	5, 10, 11, 12, 13
M5	0.05	14.29	−1.58	8, 14
M4	0.36	12.74	−1.46	15, 16
M10	0.26	14.05	−1.70	8, 17
NGC 6397	0.18	12.3	−2.24	3, 18, 19
M22	0.35	13.8	−1.86	19, 20, 21
NGC 6752	0.05	13.0	−1.52	3, 19, 22
M15	0.12	14.88	−2.15	8, 23
NGC 7099	0.06	14.60	−2.26	8, 24
M67	0.06	9.56	+0.11	25, 26
Mel 66	0.17	12.91	−0.3	26, 27
NGC 2243	0.04	13.03	−0.7	28, 29

REFERENCES.—(1) Lee 1977*b*. (2) Dickens *et al.* 1979. (3) Cannon 1974. (4) Menzies 1967 (see Alcaino 1973). (5) Eggen 1972. (6) Alcaino 1976. (7) McClure and Norris 1974. (8) Kukarkin 1974. (9) Lee 1977*c*. (10) Woolley 1966. (11) Cannon and Stobie 1973*a*. (12) Dickens and Bell 1976. (13) Butler *et al.* 1978. (14) Arp 1962. (15) Lee 1977*a*. (16) Cacciari 1979. (17) Harris *et al.* 1976. (18) Woolley *et al.* 1961. (19) Mallia 1977. (20) Lloyd Evans 1975. (21) Hesser *et al.* 1977. (22) Cannon and Stobie 1973*b*. (23) Sandage 1970. (24) Dickens 1972. (25) Eggen and Sandage 1964. (26) Hawarden 1976. (27) Hawarden 1978. (28) Norris and Hawarden 1978. (29) Hawarden 1975.

observed are listed in Table 2. They are mostly close to the top of their respective giant branches, but fainter stars along the RGB have been observed when possible, in order to cover a good range in luminosity. The field red giants ε Tel and 110 Vir were also observed. The first two columns of Table 2 give the cluster and the star name. In the third column, the word yes means that Hα emission has been detected. The fourth and fifth columns give the values of V and $B-V$. The next five columns give the gravity, temperature, and luminosity calculated with the procedure described in § III*a*. The eleventh column gives log H_0, where H_0 is the FWHM of the apparent Hα absorption feature for stars with no detected Hα emission (see § IV*c*). The final column gives the residual intensity R_c for the apparent Hα absorption profile. Values of H_0 and R_c for the emission stars are given in Table 3.

For the stars in ω Cen, the values of V and $B-V$ which were taken from Woolley (1966) have been increased by 0.04 and decreased by 0.07 respectively, as suggested by Cannon and Stobie (1973*a*). In NGC 3201 the star 1207 was found to be a nonmember and has not been included in Table 2. The stars in which some direct evidence of Hα emission was found are listed in Table 3. For a detailed description of the spectroscopic data, see § III*b*.

III. RESULTS

a) Physical Parameters

For the discussion in § IV, we will need effective temperatures and bolometric corrections for our stars. The colors $(V-K)$ and $(R-I)$ are believed to be good temperature indicators (Cohen, Frogel, and Persson 1978; Persson *et al.* 1980; Dickens and Bell 1976), but unfortunately they are not available for all the stars that we have observed. The $(B-V)$ colors can also be fairly good temperature indicators, provided that some information is available about gravity and metal abundance, so we have used them together with Bell and Gustafsson's (1978) atmospheric models for cool stars to calculate the values of effective temperature listed in the sixth column of Table 2. When it was necessary to interpolate or extrapolate in the model grid, we assumed the same shape for the $(B-V)_0$–T_e and B.C.–T_e functions as for Johnson's (1966) relations for normal giants.

The procedure to calculate $T_e(B-V)$ was as follows. Starting with the value of [Fe/H] appropriate for that cluster (see Table 1) and a reasonable first guess at the gravity of the star, we determined from $(B-V)_0$ the first estimate of T_e and B.C., which allowed us to calculate a new value of g. This value was then used again in an iterative procedure which was continued until it converged. We assumed $M_{bol} = 4.75$ for the Sun (Allen 1973) and $M = 0.8\ M_\odot$ for all our stars. For the stars in ω Cen for which no specific measure of [Fe/H] was available, the average value −1.5 was used. This procedure could not be used for the stars III-11 and III-70 in NGC 362 because their very red $B-V$ colors would have required a very large extrapolation in the model atmosphere grid.

For the stars for which the $(R-I)_K$ colors are available, an alternative temperature $T_e(R-I)$ was obtained using the temperature scale of Johnson (1966) for normal giants[2] and assuming the transformation equation given by Eggen (1972). The reddening was taken to be $E(R-I) = 0.7E(B-V)$ (Eggen 1974). The temperature adopted for these stars was the mean of $T_e(B-V)$ and $T_e(R-I)$, rounded off to 50 K. In all cases the temperature adopted did not differ by more than 100 K from $T_e(B-V)$; therefore, when $T_e(R-I)$ was not available, the value of $T_e(B-V)$ was adopted, without attempting to introduce any correction which would probably be within the errors of the procedure.

An error of 0.05 in $B-V$ and $R-I$ gives an error of about 70 K and 100 K, respectively, in T_e. The uncertainty in log g resulting from an error of 100 K in T_e is about 0.09, while an error of 0.1 mag in the determination of M_V [from $E(B-V)$, V, and the distance modulus] gives an error of 0.04 in log g. We estimate that the errors in our adopted values for T_e and log g are unlikely to exceed 100 K and 0.1, respectively, except in the cases where the photometry is uncertain

[2] The temperature scale of Dickens and Bell 1976, using Bell and Gustafsson's 1975 models, gives essentially the same temperatures as Johnson's scale for $(R-I)_0 < 0.5$, but lower temperatures by up to 200 K for $(R-I)_0 > 0.5$. In their most recent calculations, Bell and Gustafsson 1978 do not give results for *RIJK* photometry. Therefore, we have chosen to use the empirical temperature scale defined by Johnson 1966 for normal giants, relying on the fact that the $(R-I)$–T_e relation is not very sensitive to metal abundance.

TABLE 2

ATMOSPHERIC PARAMETERS FOR ALL THE STARS OBSERVED IN THIS SURVEY

Cluster	Star	Em.	V[a]	B-V[a]	T_e(B-V)	T_e(R-I)[b]	T_e(adop)[c]	log g	log $L/L_\odot$	log H_o	R_c
47 Tuc	3512		11.79	1.63	3800			0.6	3.01	0.01	0.291
	1205		11.85	1.61	3800			0.6	2.99	0.07	0.262
	1603		11.89	1.58	3850			0.7	2.95	0.09	0.205
	5529		11.89	1.59	3850			0.7	2.95	0.13	0.232
	2426		12.10	1.52	3900			0.8	2.84	0.09	0.243
	3501		12.13	1.47	3950			0.9	2.81	0.08	0.298
	4603		12.13	1.41	4000			0.9	2.79	0.14	0.214
	1510		12.15	1.43	4000			0.9	2.78	0.13	0.046
	4418		12.16	1.46	3950			0.9	2.80		
	1505		12.16	1.50	3900			0.8	2.82	0.30	0.295
	5312		12.18	1.49	3900			0.8	2.81	0.05	0.300
	5309		12.20	1.49	3900			0.9	2.80	0.13	0.228
NGC 362	III-11	yes	12.11	2.17							
	III-39		12.67	1.58	3900	3970	3950	0.5	3.14	-0.07	0.539
	III-70		12.53	1.71						0.20	0.333
	IV-84		12.94	1.50	3950	4100	4050	0.7	2.99	-0.05	0.500
NGC 3201	1312		11.77	1.74	3900			0.4	3.26	0.14	0.148
	1314		11.77	1.53	4150			0.6	3.15	0.11	0.216
	1117		11.93	1.60	4050			0.6	3.12	0.11	0.180
	4524	yes	11.97	1.57	4100			0.7	3.09		
	3204		12.29	1.44	4250			0.9	2.90	0.12	0.303
	3218		12.37	1.57	4100			0.8	2.93	0.11	0.181
ω Cen	ROA 40	yes?	11.37	1.50	4100	4070	4100	0.5	3.22		
	41		11.44	1.29	4400			0.7	3.09	0.11	0.268
	42	yes	11.44	1.55	4050			0.5	3.21		
	43		11.64	1.71	3850	4000	3950	0.5	3.17	0.02	0.232
	44	yes	11.46	1.25	4400			0.8	3.08		
	45		11.46	1.42	4200			0.6	3.14	0.08	0.216
	49	yes	11.58	1.59	4000			0.5	3.18		
	51		11.50	1.51	4050			0.5	3.19	0.09	0.203
	52	yes	11.50	1.48	4150			0.6	3.15		
	53	yes	11.58	1.70	3850	3970	3900	0.4	3.22		
	54	yes	11.52	1.44	4200			0.7	3.12		
	56		11.70	1.65	3950	3940	3950	0.5	3.15	-0.01	0.185
	58		11.64	1.42	4200	4010	4100	0.6	3.11	0.13	0.180
	63		11.57	1.30	4350			0.8	3.05	0.11	0.184
	64		11.57	1.32	4350			0.8	3.05	0.07	0.189
	65	yes	11.61	1.50	4100	4080	4100	0.6	3.12		
	66	yes	11.53	1.62	3950	3940	3950	0.5	3.22		
	67		11.64	1.51	4100	4110	4100	0.6	3.11	0.08	0.199
	69		11.61	1.39	4250			0.7	3.07	0.02	0.206
	71		11.63	1.49	4100			0.6	3.12	0.13	0.180
	73	yes	11.70	1.64	3950	3940	3950	0.5	3.15		
	74		11.74	1.36	4250	4120	4200	0.8	3.03	0.09	0.147
	75	yes	11.65	1.35	4300			0.8	3.04		
	76	yes	11.65	1.25	4400			0.9	3.01		
	77		11.67	1.30	4350			0.8	3.01	0.08	0.248
	78		11.67	1.22	4450			0.9	2.98	0.05	0.254
	79	yes	11.69	1.31	4350			0.8	3.00		
	81		11.70	1.18	4500			0.9	2.96	0.07	0.223
	82		11.70	1.44	4150			0.7	3.07	0.09	0.150
	84		11.87	1.66	3900			0.5	3.10	-0.02	0.220
	85		11.84	1.61	3950			0.6	3.09	0.08	0.058
	86		11.71	1.16	4500			1.0	2.96	0.05	0.238
	89		11.73	1.47	4100			0.7	3.07	0.08	0.104
	90		11.66	1.64	3950			0.5	3.16		
	91		11.81	1.39	4200	4110	4150	0.7	3.02	0.18	0.245
	92		11.74	1.53	4050			0.6	3.09	0.02	0.000
	94	yes?	11.80	1.40	4200	4080	4150	0.7	3.03		
	95		11.77	1.62	3950	3980	3950	0.6	3.12	0.07	0.189
	96		11.76	1.48	4100	4120	4100	0.7	3.06	-0.01	0.229
	97		11.76	1.29	4350			0.9	2.98	0.13	0.252
	99		11.78	1.38	4250			0.8	3.00		
	100	yes	11.74	1.60	4000			0.6	3.11		
	101		11.78	1.07	4600			1.0	2.94	0.13	0.218
	102	yes	11.68	1.46	4150	4100	4100	0.7	3.09		
	104		11.79	1.36	4250			0.8	3.00	-0.05	0.000
	105	yes	11.79	1.37	4250			0.8	3.00		
	106		11.79	1.24	4400			0.9	2.95	0.04	0.170
	108	yes	11.80	1.56	4000			0.6	3.09		
	109		11.80	1.33	4300	4120	4200	0.8	3.01	0.02	0.063
	110		11.80	1.39	4200			0.8	3.01	0.05	0.188
	111		11.80	1.32	4300			0.8	2.98	0.08	0.120
	115		11.81	1.29	4350			0.9	2.96	0.08	0.243
	117		11.82	1.37	4250			0.8	2.98	0.05	0.205
	119		11.84	1.44	4150			0.7	3.01	0.10	0.214
	120	yes?	11.85	1.24	4400			0.9	2.93		
	122		11.85	1.30	4350			0.9	2.94	0.08	0.203
	123		11.85	1.16	4500			1.0	2.90	0.16	0.221
M5	I-68		12.30	1.58	3900	4000	3950	0.6	3.05	0.02	0.138
	II-85		12.31	1.54	3950			0.6	3.05	0.05	0.189
	IV-47		12.33	1.51	3950	4020	4000	0.7	3.01	0.05	0.157
	IV-81		12.10	1.59	3900			0.5	3.16	0.06	0.164
M4	4613	yes?	10.81	1.97	3650	3840	3750	0.5	3.11		
	1514		10.85	1.85	3850	3860	3850	0.6	3.05	0.08	0.181
	4611	yes	11.02	2.00	3600	3820	3700	0.5	3.05		

TABLE 2—*Continued*

Cluster	Star	Em.	V[a]	B-V[a]	T_e(B-V)	T_e(R-I)[b]	T_e(adop)[c]	log g	log $L/L_\odot$	log H_o	R_c
M10	I- 15		12.30	1.47	4250			1.0	2.84	0.11	0.248
	I-285		12.73	1.43	4300			1.2	2.65		
	I-367		12.27	1.51	4200			0.9	2.87		
	II-44		11.87	1.60	4100			0.7	3.07	0.08	0.195
	II-161		12.64	1.48	4250			1.1	2.70		
	II-217		12.75	1.43	4300			1.2	2.64	0.18	0.329
NGC 6397	28		11.81	.94	4850			1.8	2.20	0.18	0.324
	43		10.94	1.12	4650			1.4	2.58	0.13	0.239
	75		12.12	.87	4950			2.0	2.06	0.18	0.304
	99		10.74	1.26	4450			1.2	2.71	0.17	0.233
	211	yes	10.16	1.46	4200			0.8	3.02		
	420		11.50	1.05	4700			1.6	2.34	0.15	0.279
	459		11.16	1.10	4650			1.5	2.49	0.08	0.276
	468		11.50	1.05	4700			1.6	2.34	0.13	0.265
	469	yes	9.96	1.51	4150			0.6	3.12		
	603		10.35	1.33	4350			0.9	2.90	0.08	0.234
	669		10.50	1.28	4400			1.0	2.82	0.11	0.243
	685		12.01	.97	4800			1.9	2.12	0.19	0.248
	698		10.28	1.50	4150			0.8	3.00	0.04	0.218
	708		11.50	1.09	4650			1.6	2.36	0.16	0.273
M22	II-26	yes	11.42	1.64	4250	4160	4200	0.7	3.10		
	II-67	yes?	11.40	1.69	4200			0.6	3.13		
	II-80		11.59	1.71	4200			0.7	3.05	0.08	0.167
	III-3	yes	11.27	1.78	4100	4120	4100	0.5	3.22		
	III-14		11.26	1.76	4100	4020	4050	0.5	3.22	-0.01	0.230
	III-15	yes?	11.36	1.68	4200			0.6	3.14		
	III-26	yes	11.30	1.71	4200			0.6	3.17		
	IV-17	yes	11.45	1.79	4100			0.6	3.14		
	IV-97		11.08	1.86	4000	4090	4050	0.4	3.30	0.02	0.279
	IV-102	yes?	10.99	1.78	4100	4110	4100	0.4	3.33		
NGC 6752	A3		12.02	1.09	4550			1.5	2.45	0.13	0.116
	A8		12.03	1.12	4450	4430	4450	1.4	2.47	0.13	0.145
	A9		11.30	1.20	4350			1.1	2.79	0.08	0.233
	A12		11.25	1.35	4150	4140	4150	0.9	2.87	0.08	0.226
	A29		11.85	1.14	4400	4320	4350	1.3	2.56	0.11	0.154
	A30		12.18	1.06	4500	4700	4600	1.6	2.37	0.18	0.219
	A31	yes	10.80	1.60	3950	3920	3950	0.5	3.13		
	A36		11.59	1.16	4400			1.2	2.66	0.18	0.188
	A45		11.57	1.23	4300	4240	4250	1.1	2.70	0.12	0.315
	A59	yes	10.90	1.59	3950	3950	3950	0.6	3.09		
	A61		11.71	1.13	4450			1.3	2.60	0.08	0.211
	A68		12.02	1.11	4450	4430	4450	1.4	2.47	0.16	0.166
	3		11.50	1.25	4300			1.1	2.72	0.13	0.226
	135		11.44	1.15	4450			1.2	2.70	0.11	0.164
M15	S4		12.69	1.37	4250			0.8	3.03	-0.02	0.251
NGC 7099	Pe23	yes	12.20	1.40	4200			0.6	3.12		
Mel 66	2239		11.80	1.58	4000			1.0	2.67	0.22	0.294
	2206		12.63	1.46	4200			1.5	2.27	0.10	0.194
	4151		12.69	1.56	4000			1.4	2.32	0.23	0.328
NGC 2243	4209		12.03	1.43	4000			1.0	2.63	0.17	0.227
	4110		12.85	1.11	4300			1.6	2.19	0.13	0.189
M67	105		10.30	1.26	4300	4270	4300	2.0	1.82	0.13	0.233
	108		9.72	1.37	4100	4120	4100	1.6	2.12		
	141		10.48	1.11	4600	4550	4600	2.3	1.68	0.17	0.272
	151		10.53	1.09	4600	4660	4650	2.3	1.65	0.16	0.233
	170		9.69	1.36	4100	4120	4100	1.6	2.14	0.13	0.247
	266		10.55	1.11	4600	4660	4650	2.3	1.64	0.16	0.259
	ε Tel[d]		4.52	1.01	4760				1.78	0.17	0.263
	110 Vir[d]		4.40	1.04	4720				1.80	0.11	0.235

[a] Sources are the same as in Table 1.
[b] Sources of $(R-I)$ are Bessell and Norris 1976 for ω Cen ROA 53 and ROA 102; otherwise Eggen 1972.
[c] When no T_e adopted is indicated, it means that $T_e(B-V)$ has been adopted.
[d] Sources are Hoffleit 1964 for V and $B-V$, and Johnson 1966 and Allen 1973 for $T_{\rm eff}$ and L derived from stars of the same spectral type.

and/or the atmospheric models had to be extrapolated ($T_e < 4000$ K).

b) *Spectroscopic Data and Mass Loss*

The results of our spectroscopic survey are presented in Table 3, where the stars showing Hα emission above the level of the continuum are listed. The column labeled "Em" indicates the kind of emission (to the red or blue of the Hα absorption feature) seen in the raw spectrum. The W_λ column gives the equivalent width of the emission component(s) (see below), $V(E-A)$ is the velocity shift between the Hα emission and absorption components, and $\dot{M}$ is an estimate of the mass loss rate.

In determining W_λ the following empirical procedure has been adopted in order to take account of the part of the emission profile falling within the absorption line.

TABLE 3

SPECTROSCOPIC DATA FOR THE STARS WITH Hα EMISSION

Cluster	Star	Date	Em.	W_λ (Å)	V_{E-A} (km sec^{-1})	Log H_o	R_c	M (10^{-8} $M_\odot$ yr^{-1})	Remarks
NGC 362	III-11	20.10.78	B	0.07	-46	-0.10	0.292		
NGC3201	4524	8. 3.79	R,B	0.86	+40,-46	-0.17	0.260	5.2	Var 79
ω Cen	ROA 40	6. 2.79				0.09	0.190		
		13. 7.79	B?	0.02	-63		0.189	1.6	
	42	6. 3.79	R,B	0.10	+49,-59	-0.01	0.255	2.9	
	44	5. 3.79	B?	0.01	-55	0.05	0.168	0.7	
		14. 7.79	B?			0.01	0.176		
	49	4. 3.79	R	0.15	+53	0.01	0.304	3.4	Var
	52	7. 4.79	R,B	0.37	+46,-56	-0.13	0.311	4.7	
		9. 5.79	R,B	0.18,0.07	+56,-58	-0.06	0.264	4.3	
		14. 5.79	R,B?	0.16	+46	-0.06	0.224	2.8	
		15. 5.79	R,B	0.24,0.06	+58,-61	-0.03	0.234	5.0	
		8. 6.79	R,B	0.73	+42,-53	-0.17	0.332	6.1	
		9. 6.79	R,B	0.62	+49,-53	-0.16	0.362	6.1	
		10. 6.79	R,B	0.53	+46,-46	-0.17	0.322	5.1	
		10. 7.79	R,B	0.73	+45,-45	-0.29	0.365	5.9	
		13. 7.79	R,B	0.80	+45,-47	-0.24	0.400	6.3	
	53	5. 3.79	R	0.05	+59	-0.06	0.215	2.4	Var
	54	7. 4.79	R	0.09	+53	0.02	0.184	2.2	
		14.7.79	B	0.05	-51	-0.01	0.218	1.6	
	65	10. 7.78	B	0.11	-59	0.01	0.243	2.9	
		5. 2.79	R	0.04	+52	-0.01	0.256	1.5	
		6. 3.79	R	0.10	+55	-0.06	0.233	2.6	
		4. 5.79	R,B	0.14,0.12	+44,-49	-0.09	0.208	3.5	
		9. 5.79	R,B	0.12,0.05	+53,-57	-0.02	0.210	3.3	
		13. 5.79	R,B	0.10,0.09	+51,-66	-0.02	0.265	3.7	
		14. 5.79	R,B	0.10,0.14	+46,-46	-0.02	0.225	3.3	
		8. 6.79	R,B	0.14,0.14	+53,-53	-0.07	0.238	4.1	
		9. 6.79	R,B	0.09,0.10	+46,-49	-0.06	0.219	3.1	
		10. 6.79	R,B	0.14,0.18	+63,-59	-0.06	0.248	5.1	
		14. 7.79	R,B	0.02,0.03	+53,-49	-0.05	0.192	1.7	
		15. 7.79	R,B	0.06,0.09	+51,-53	-0.06	0.206	3.0	
	66	6. 2.79	R	0.07	+53	-0.02	0.284	2.3	
	73	8. 3.79	R	0.09	+53	-0.06	0.235	2.5	
	75	8. 3.79	B	0.07	-51	0.05	0.202	1.6	
	76	9. 3.79	R	0.06	+63	0.08	0.171	1.8	
	79	7. 4.79	B	0.07	-65	0.05	0.196	2.1	
	94	9. 3.79	R?			0.03	0.178		
	100	15. 5.79	B	0.07	-65	0.08	0.132	2.4	
	102	14. 5.79	B	0.07	-53	-0.06	0.220	1.8	
	105	14. 5.79				0.00	0.200		
		15. 5.79	R	0.05	+51	-0.04	0.192	1.3	
	108	15. 5.79	R	0.04	+46	-0.06	0.194	1.3	
	120	10. 7.79	R?	0.03	+56		0.213	1.0	
M4	4613	8. 4.79	B?	0.01	-76	0.03	0.175	1.1	
	4611	8. 4.79	B	0.09	-66	-0.02	0.212	2.6	
NGC 6397	211	12. 7.78	R,B	0.08	+61,-56	0.02	0.231	1.9	
	469	12. 7.78	R,B	0.08	+61,-59	0.01	0.243	2.5	
M22	II-26	14. 7.79	B	0.04	-63	0.10	0.187	1.7	
	II-67	23. 8.78	B?	0.02	-69	0.02	0.304	1.5	
	III-3	20.10.78	B	0.07	-76	0.01	0.294	3.5	
	III-15	20.10.78	B?	0.02	-61	0.08	0.220	1.3	
	III-26	16. 7.78	R,B	0.04,0.06	+53,-56	0.02	0.218	2.7	
		20.10.78				0.09	0.225		
	IV-17	23. 8.78	R,B	0.09,0.08	+72,-53	-0.03	0.259	3.8	
	IV-102	13. 7.79	R?			0.05	0.172		
NGC 6752	A31	14. 7.78	R,B	0.39	+46,-49	-0.10	0.297	4.6	
		23. 8.78	R,B	0.23	+49,-59	-0.09	0.269	4.0	
		4. 5.79	R,B	0.09,0.05	+54,-53	-0.04	0.216	3.1	
		13. 5.79	R,B	0.43	+45,-46	-0.14	0.286	4.6	
		15. 5.79	R,B	0.50	+46,-46	-0.16	0.307	5.0	
		8. 6.79	R	0.16	+53	-0.06	0.257	3.2	
		9. 6.79	R	0.16	+49	-0.05	0.252	3.0	
	A59	13. 7.78	R,B	0.06,0.03	+53,-56	0.02	0.223	2.3	
NGC 7099	Pe23	20.10.78	R	0.08	+53	-0.03	0.215	2.3	

If the emission was not too strong and only on one side of the absorption line, then the half-profile which showed no emission was used to derive a "mean" profile which was then subtracted from the observed one. If the emission was strong and/or on both sides of the absorption line, then another star from the same cluster was chosen, with no Hα emission and with values of V and $B-V$ as close as possible to those for the emission star. Its absorption profile was then subtracted from the observed one, on the assumption that stars with the same physical parameters have similar Hα absorption profiles. Typical errors in the W_λ values, from placement of the continuum level and determination of the line profile are about 10%–20% for $W_\lambda > 0.1$ Å and up to 30%–50% for $W_\lambda < 0.1$ Å. For the equivalent width W_λ of the Hα emission given in Table 3, there are one or two values,

depending on whether the *net* Hα profile (after subtraction according to the procedure just described) showed one or two distinct emission peaks.

Following Cohen (1976) and Mallia and Pagel (1978), we assume that the Hα emission we have detected arises from an expanding circumstellar envelope formed from mass lost by the star. In the absence of detailed knowledge of the structure and excitation mechanism of this region of the star, the recombination model of Cohen (1976) is a first approximation. According to this model, the mass loss rate is given by

$$\dot{M} = 2.4 \times 10^{-11} V_{\rm exp} R_* (R_s W_\lambda)^{1/2} \times \exp(-1.1/T_4)\, M_\odot\ {\rm yr}^{-1}, \quad (1)$$

where $V_{\rm exp}$ is in km s^{-1}, R_* and R_s in solar radii, W_λ in Å, and T_4 in units of 10^4 K. The expansion velocity $V_{\rm exp}$ of the shell is assumed to be uniform; in our computations the values of $V(E-A)$ from Table 3 (or their mean value where more than one is available) have been used. The shell has been assumed to have a base level of radius $R_s = 2R_*$, where R_* is the radius of the star. The values of the mass loss rate derived from equation (1) are listed in the seventh column of Table 3. They are only a rough estimate of the true rate, which could easily be different by an order of magnitude, due to the crude approximations in the theoretical model and to the uncertainties in some of the quantities appearing in equation (1).

IV. DISCUSSION

a) Mass Loss in the H-R Diagram

Using the value of temperature and luminosity listed in Table 2, we have plotted the H-R diagram of all our stars in Figures 1*a* and 1*b*. The two theoretical isochrones from Bertelli *et al.* (1979) correspond to age = 12×10^9 yr, $X = 0.7$, $Z = 0.0004$, and $Z = 0.004$.

As already noted by Cohen, Frogel, and Persson (1978) and Persson *et al.* (1980), we also find that the slopes of the cluster giant branches are flatter than the theoretical tracks. This cannot be due to the presence of AGB stars, because in our sample there are only three or four such stars (stars 28, 75, and possibly 685 in NGC 6397, and star 135 in NGC 6752).

From Figure 1 and Table 2, a few conclusions can be drawn. (1) There is no evidence for emission, at our threshold of detection, below about log $(L/L_\odot) = 2.9$. (2) For stars with log $(L/L_\odot) > 2.9$, only about one-third show emission. There is weak evidence that these emission stars occur preferentially in the hottest stars, which belong to the most metal-weak clusters. (3) In the chemically inhomogeneous cluster ω Cen, there is, however, no evidence for preferential emission in the metal weakest stars. Figure 1*b* shows that Hα emission occurs all across the wide giant branch, with no apparent correlation with temperature or metal abundance. We can also show that the Hα emission for these stars does

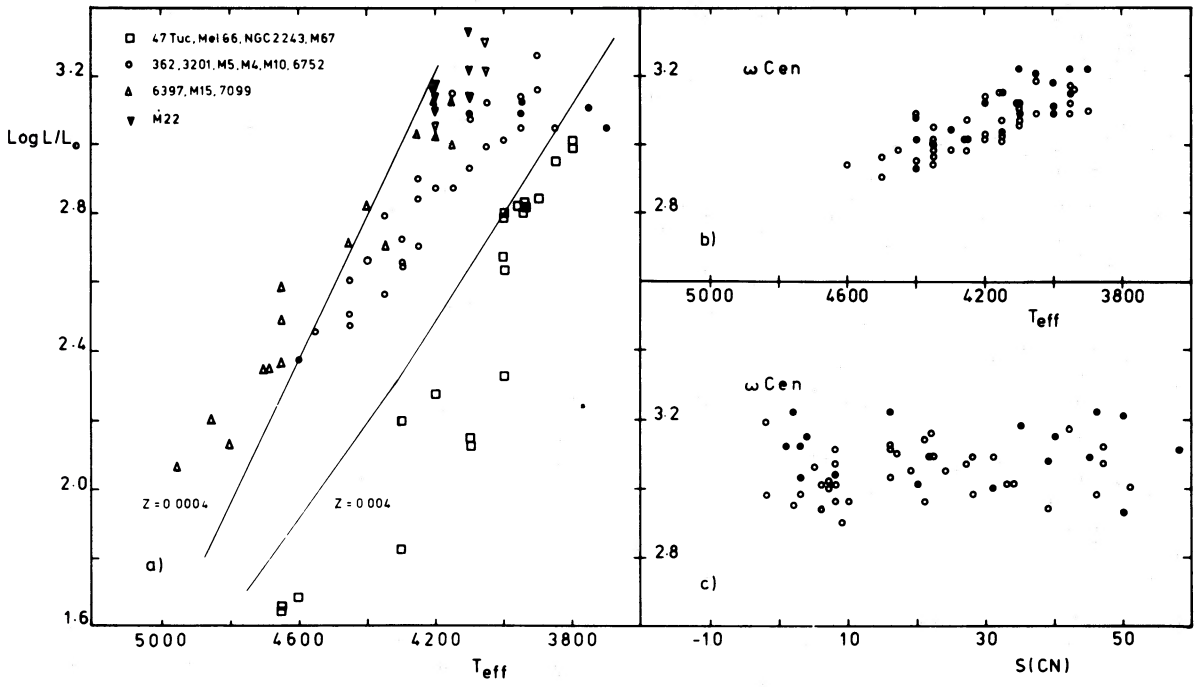

FIG. 1.—Fig. 1*a* is the H-R diagram for the stars observed in this survey. Stars in ω Cen are shown separately in Fig. 1*b*. Values of T_e and log $(L/L_\odot)$ come from Table 2. Different symbols indicate clusters of different metallicity; filled symbols represent stars in which Hα emission above the continuum level has been detected. The two theoretical isochrones from Bertelli *et al.* 1979 correspond to age = 12×10^9 yr, $X = 0.7$, and $Z = 4 \times 10^{-4}$, 4×10^{-3}. Fig. 1*c* shows the CN index $S(3839)$ against log $(L/L_\odot)$ for the ω Cen stars plotted in Fig. 1*b*: the strength of the violet CN feature increases with $S(3839)$.

not correlate with the strength of the violet CN feature, which is known to vary greatly from star to star in ω Cen. Figure 1*c* shows the CN index S(3839) for our ω Cen stars, from Norris, Freeman, and Seitzer (1983). No dependence of emission on CN strength is seen. Peterson (1982) reached a similar conclusion, that there is no clear dependence of mass loss on metallicity.

These observations are consistent with the dependence of mass loss rate on luminosity found by Reimers (1975, 1977) for Population I red giants, and with the theoretical stellar wind model proposed by Fusi Pecci and Renzini (1975). If we set $\dot{M} = 10^{-8}\ M_\odot\ \mathrm{yr}^{-1}$ as a lower limit of detectability of mass loss through Hα emission according to the assumptions and parameters used in this paper, then Reimer's relation gives a lower limit to the luminosity of $\log (L/L_\odot) = 2.8$ which is approximately the threshold we observe in Figure 1. It would be interesting to obtain more observations of fainter stars to check further the dependence of the Hα emission (or mass loss rate) on luminosity.

The fact that in many cases no Hα emission is seen in stars very similar in luminosity, radius, and composition to others showing Hα emission has been commented on already by Mallia and Pagel (1978). Only a small scatter in the mass loss rate around the value predicted by the theory would be sufficient to produce a rate below the level of detectability, due to the dependence of W_λ on $\dot{M}^2$ in equation (1). Furthermore, there is now ample evidence (see next section) that the mass loss can be variable in time. Both these facts, and the stronger dependence of $\dot{M}$ on L than on Z, can be responsible for the apparent lack of correlation between Hα emission and position of the stars in the H-R diagram of ω Cen.

b) Time Variability of Hα *Emission*

In order to check for Hα emission variability, a few stars have been observed several times. The journal of the observations is given in Table 3. It is immediately evident that the emission components in the Hα profile are not constant with time and can vary appreciably even over only a few days. A few examples: star 65 in ω Cen showed stronger emission in the red than in the blue on 1979 May 9, and only 5 days later the situation was reversed. On 1979 July 14 the emission was very weak on both sides, while 1 month earlier it was quite strong on both sides. Star A31 in NGC 6752, which had quite strong red and blue emission in 1979 mid-May, showed only red emission in 1979 June.

A comparison of our data with Mallia and Pagel's (1978) and Cohen's (1981) data confirms the variability of the Hα profile for the stars 211 in NGC 6397, III-14 and IV-97 in M22, and ROA 58 and 102 in ω Cen. A similar kind of variation has been found by Ramsey (1979) in the metal-poor field red giant HDE 232078. The time scale of these variations can be only a few days. Whether this a geometrical effect or a real variation in the mass loss rate is not yet clear. In the latter case, the recombination time of hydrogen must be smaller than the time scale of the variation of the emission profile, for the variation itself to be visible.[3] A typical recombination time is $t_r = 10^5 N_e^{-1}\ \mathrm{yr}^{-1}$ (Osterbrock 1974), where N_e is the electron density in cm^{-3}. This leads to a lower limit on the mass loss rate of about $10^{-10}\ M_\odot\ \mathrm{yr}^{-1}$, for a variation time of about 1 month and for typical values of the circumstellar shell radius $R_s = 2R_* = 140\ R_\odot$, and an expansion velocity $V_{\mathrm{exp}} = 50\ \mathrm{km\ s}^{-1}$. This lower limit is consistent with the estimates of mass loss rates (about $2\text{–}5 \times 10^{-8}\ M_\odot\ \mathrm{yr}^{-1}$) which we have derived using Cohen's (1976) approximations. Both these estimates are however uncertain by at least an order of magnitude, because of the approximations used. In particular, the actual values of the mass loss rates could be much larger, because the ionized hydrogen could be only a few percent of the total hydrogen in the shell. Moreover, the mass loss estimates could represent only a sporadic mass loss, and should not be used in evolutionary calculations.

The discussion in § IV*a* remains statistically valid, because it is based on a fairly large number of stars, but should not of course be applied to any individual star.

c) The Luminosity-FWHM Relation

In the last two sections, we showed that Hα emission is visible (i.e., appears above the level of the continuum) only in some giants with $\log (L/L_\odot) > 2.9$. Even for these giants, the Hα emission appears to be variable. Weaker emission, that does not appear above the level of the continuum, could however be present in fainter stars. We will now discuss evidence for such weak Hα emission in some giants with $\log (L/L_\odot)$ as faint as 2.3 ($M_{\mathrm{bol}} = -1.0$).

Weak redshifted or blueshifted Hα emission will reduce the apparent width of the Hα absorption line. To see whether such narrowing is present for some of our stars in which no Hα emission was measured directly, we measured the full width at half-maximum H_0 of the Hα absorption line for those stars in which Hα emission above the level of the continuum was not detected. (H_0 has been corrected for instrumental broadening, using the relation $H_0^2 = H^2 - \delta^2$, where H is the observed FWHM and δ is the FWHM of the instrumental profile; see § II.) Figure 2 shows $\log H_0$ against M_{bol}; there is a clear trend of decreasing $\log H_0$ and increasing scatter in $\log H_0$ with decreasing (brighter) M_{bol}.

This trend of $\log H_0$ with M_{bol} is in the opposite sense to that reported for late-type Population I stars by Kraft, Preston, and Wolff (1964) and Lo Presto (1971). Figure 3 shows the $\log H_0$–M_{bol} diagram for a recent homogeneous sample of late-type Population I stars. (We are indebted to Mr. D. Zarro for allowing us to use this data before publication.) The region of the plane occupied by our globular cluster giants is also shown, for comparison; the opposite senses of the trends for Population I and Population II stars are fairly evident. However the Population I sample includes stars

[3] We are grateful to D. Reimers for this comment.

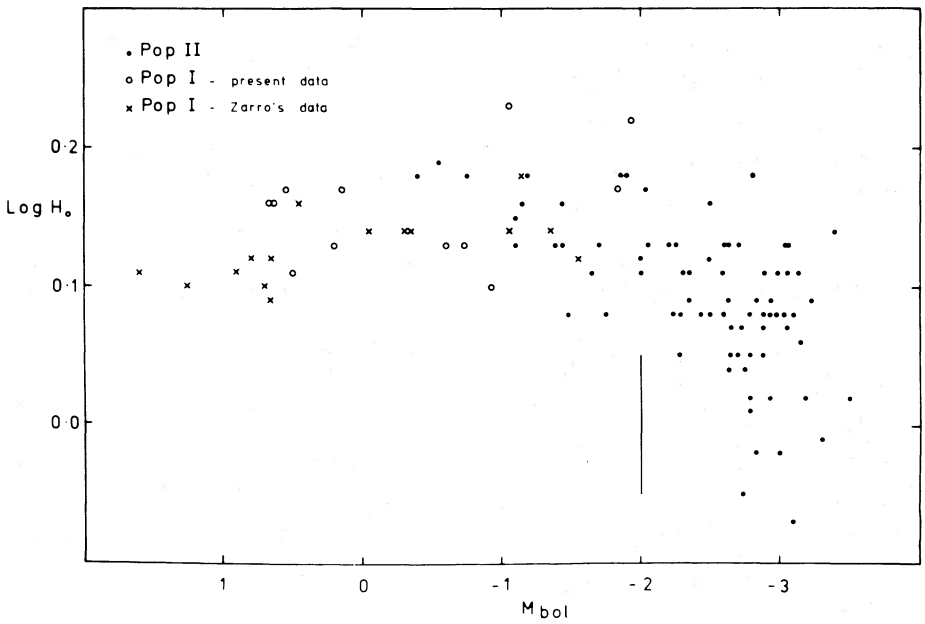

FIG. 2.—Log H_0 against M_{bol} for the red giants of our survey which did not show Hα emission above the continuum, and for the Population I red giants with $M \approx 1\ M_\odot$ from Zarro's sample. H_0 is the corrected FWHM for the Hα absorption feature. The vertical line at $M_{bol} = -2$ represents the luminosity threshold above which Reimers 1977 finds recurrent mass loss in his sample of Population I red giants.

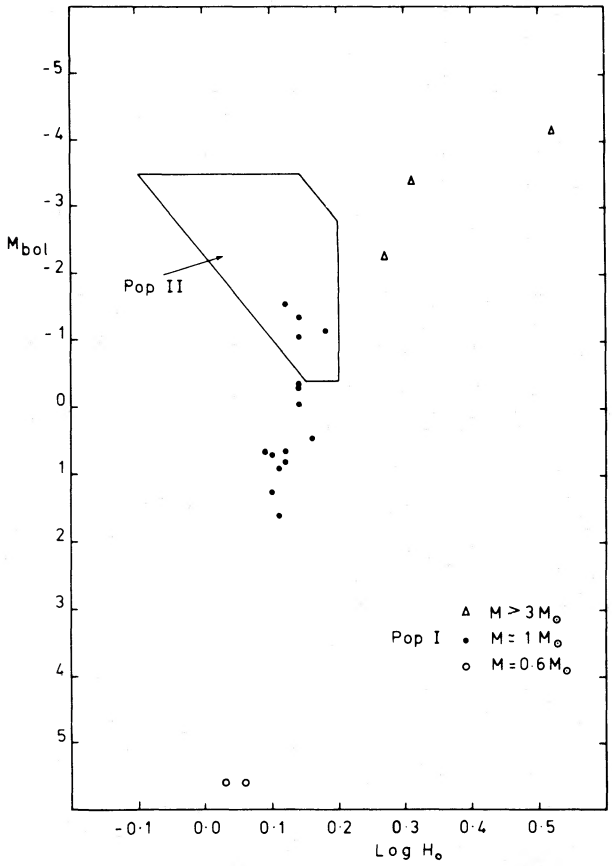

FIG. 3.—Log H_0 against M_{bol} for Zarro's sample of late-type Population I stars. Different symbols denote different stellar masses. The region of the plane occupied by our globular cluster giants is shown for comparison.

of a wide range in mass and age. For comparison with our globular cluster giants, it would be more appropriate to include only the old Population I giants with masses of about one solar mass. These stars are shown in Figure 2, together with our globular cluster and old open cluster giants. The faint end of the Population II distribution overlaps the bright end of the Population I distribution in the log H_0–M_{bol} plane. This suggests that the Hα absorption line widths are set by similar processes in this region of overlap, for low mass stars of both populations.

According to Reimer's (1977) mass loss domains for late-type Population I stars in the H-R diagram, stars of spectral types G8–K5 (similar to those in our sample) and brighter than $M_{bol} = -2$ are expected to show some evidence of recurrent mass loss. This luminosity threshold is shown in Figure 2; it is evident that the scatter in the log H_0–M_{bol} plane increases significantly for those stars brighter than this threshold. However, it also appears that the trend of decreasing H_0 with increasing luminosity begins as faint as $M_{bol} = -1$ for the Population II stars. There is no evidence for such a downturn in the log H_0–M_{bol} relation for the Population I stars in Figure 2.

What is the reason for this decrease of H_0 with increasing luminosity for the Population II stars? If we accept that the mass loss rate is variable and luminosity-dependent (Reimers 1977), then the associated Hα emission will be in many cases below the level of detectability of our observations (see §§ IV*a* and IV*b*). This undetected Hα emission will affect the profile of the net Hα absorption feature. The result will be a narrower Hα absorption core without any visible emission component above the continuum level. This effect will

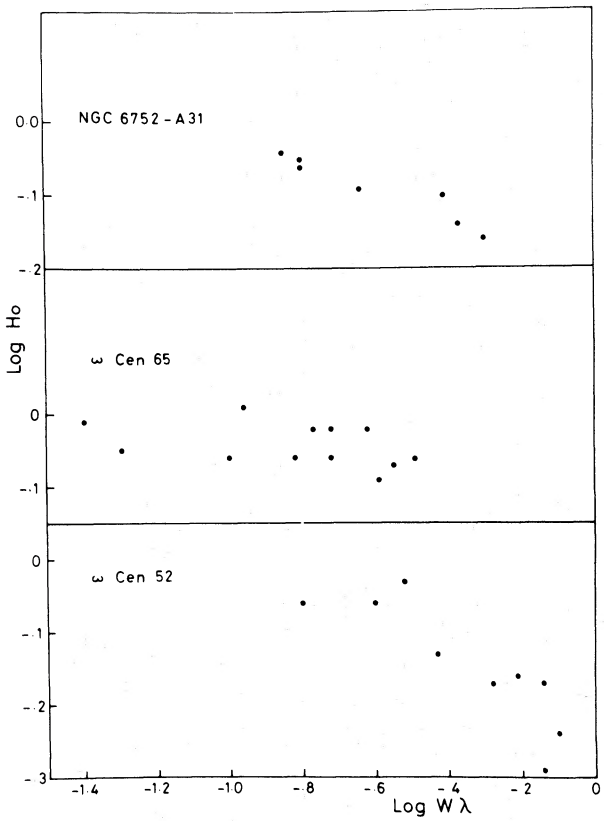

FIG. 4.—Log H_0 against W_λ for the three stars which were observed many times and which showed variability in the Hα emission. H_0 is the corrected FWHM for the apparent Hα absorption feature, and W_λ is the equivalent width of the emission components, as defined in the text.

be stronger in the mean in the brighter stars, thus producing both the trend of H_0 with M_{bol} and also the increasing scatter with increasing luminosity seen in Figure 2.

Support for this explanation comes from Figure 4, where we have plotted log H_0 (for the apparent Hα absorption feature) against the Hα *emission* equivalent width log W_λ for three stars with Hα emission that were observed many times. While star 65 in ω Cen shows no strong dependence of log H_0 on log W_λ, star 52 in ω Cen and A31 in NGC 6752 show the expected trend of narrower absorption feature for stronger emission. They all have smaller values of H_0, in any case, than the stars with no detected emission plotted in Figure 2.

As a further check on this explanation, we measured the residual intensity R_c for the apparent Hα absorption profile, in the hope that R_c would be sensitive to undetected Hα emission. (The values of R_c are given in Tables 2 and 3.) However, this was unsuccessful. Figure 5 shows the sensitivity of R_c to *detected* Hα emission. For stars having directly observed Hα emission with $W_\lambda > 0.3$ Å, the expected increase of R_c with increasing W_λ is evident. However, for stars with $W_\lambda < 0.2$, there is no significant variation of R_c with W_λ, and we cannot then expect *undetected* Hα emission to affect the R_c values significantly. If our explanation for Figure 2 is correct, it requires that the FWHM of the Hα profile (H_0) is more sensitive to undetected Hα emission than is the residual intensity R_c. From Table 3, this seems reasonable enough. We see Hα emission displaced to the red or blue by 40–70 km s^{-1} for those stars with detected Hα emission; similarly displaced undetected Hα emission would clearly affect H_0 more than R_c.

We conclude from this discussion that weak Hα emission may occur in Population II red giants as faint as $M_{bol} = -1$, and perhaps even fainter. Since we have observed few globular cluster red giants fainter than $M_{bol} = -1$, this value is an upper limit on the onset of Hα emission along the red giant branch. It seems important now to observe fainter Population II red giants, in order to define the luminosity level at which this weak Hα emission begins.

V. CONCLUSIONS

From spectra of 143 red giants in 12 globular clusters and three old open clusters, we conclude that:

1. Hα emission above the level of the continuum is seen only for some giants with log $(L/L_\odot) > 2.9$ ($M_{bol} < -2.5$). Even for these bright giants, the Hα emission appears to be variable (from our data and from comparison with the data of others).

2. From Figure 2, there may be weak Hα emission for Population II giants as faint as $M_{bol} = -1$, which is seen only by the narrowing of the apparent Hα absorption line profile.

The absence of visible Hα emission for stars of lower luminosities suggested to Peterson (1982) that mass loss along the giant branch is confined to the giant branch tip, where it is anyway a sporadic hit-or-miss process. Because of this irregularity, she argued that quiescent

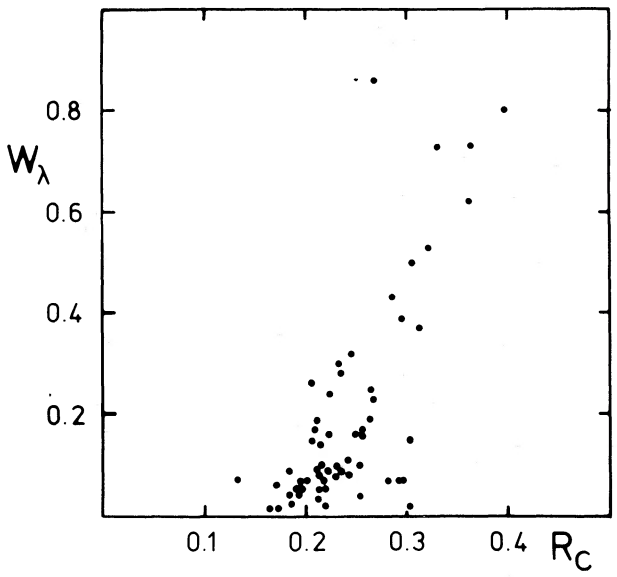

FIG. 5.—W_λ against the residual intensity R_c of the apparent Hα absorption profile, for stars with detected Hα emission.

giant branch mass loss is probably not the process responsible for a large fraction of the pre-horizontal-branch mass loss required by stellar evolution theory. More probably, it would then be responsible only for the *spread* in mass loss needed to explain the distribution of stars along the horizontal branch. Some other process would be required to explain the main part of the pre-horizontal-branch mass loss.

On the other hand, we have suggested here that weak Hα emission is found in fainter globular cluster giants also, down to at least $M_{bol} = -1$. If this weak Hα emission is as variable as the Hα emission seen directly in the brighter giants, then it seems likely that most giants brighter than about $M_{bol} = -1$ are losing mass at a mean rate of order at least $10^{-8}\ M_\odot\ yr^{-1}$. The evolutionary time from $M_{bol} = -1$ to the red giant tip for typical globular cluster giants is about 2×10^7 yr (Sweigart and Gross 1978). If we are correct so far, then this means that the total mass loss associated with the Hα emission is about $0.2\ M_\odot$, as the star evolves from $M_{bol} = -1$ to the red giant tip. This suggests that the Hα emission observed in these globular cluster giants is indeed associated not only with the *spread* in mass loss required to explain the different HB morphologies, but also with the *main part* of the pre-horizontal-branch mass loss itself.

We are very grateful to J. Cohen, L. Cram, D. Reimers, J. Norris, B. Pagel, A. Renzini, and A. Rodgers for helpful and stimulating discussions. We are particularly indebted to D. Zarro for many valuable discussions and for allowing us to use his unpublished data. Our thanks go to the staff of Mount Stromlo Observatory for support during the observations and reduction of the data. This research was carried out while one of us (C. C.) held an Australian National University Exchange Scholarship with Italy.

REFERENCES

Alcaino, G. 1973, *Atlas of Galactic Globular Clusters with Color-Magnitude Diagrams* (Santiago: Universidad Catolica de Chile).
———. 1976, *Astr. Ap. Suppl.*, **26**, 359.
Allen, C. W. 1973, *Astrophysical Quantities* (3rd ed.; London: Athlone Press).
Arp, H. C. 1962, *Ap. J.*, **135**, 311.
Bell, R. A., and Gustafsson, B. 1975, *Dudley Obs. Rept.*, **9**, 319.
———. 1978, *Astr. Ap. Suppl.*, **34**, 229.
Bertelli, G., Bolton, A., Chiosi, C., and Nasi, E. 1979, *Astr. Ap. Suppl.*, **36**, 429.
Bessell, M. S., and Norris, J. 1976, *Ap. J.*, **208**, 369.
Butler, D., Dickens, R. J., and Epps, E. 1978, *Ap. J.*, **225**, 148.
Cacciari, C. 1979, *A.J.*, **84**, 1542.
Cannon, R. D., 1974, *M.N.R.A.S.*, **167**, 551.
Cannon, R. D., and Stobie, R. S. 1973*a*, *M.N.R.A.S.*, **162**, 207.
———. 1973*b*, *M.N.R.A.S.*, **162**, 227.
Castellani, V., and Renzini, A., 1968, *Ap. Space Sci.*, **2**, 310.
Christy, R. F. 1965, *Kl. Veröff. Remeis Sternw. Bamberg*, **40**, 77.
———. 1966, *Ap. J.*, **144**, 108.
Cohen, J. G. 1976, *Ap. J.* (*Letters*), **203**, L127.
———. 1978, *Ap. J.*, **223**, 487.
———. 1979, *Ap. J.*, **231**, 751.
———. 1980, *Ap. J.*, **241**, 981.
———. 1981, *Ap. J.*, **247**, 869.
Cohen, J. G., Frogel, J. A., and Persson, S. E. 1978, *Ap. J.*, **222**, 165.
Dickens, R. J. 1972, *M.N.R.A.S.*, **157**, 299.
Dickens, R. J., and Bell, R. A. 1976, *Ap. J.*, **207**, 506.
Dickens, R. J., Bell, R. A., and Gustafsson, B. 1979, *Ap. J.*, **232**, 428.
Eggen, O. J. 1972, *Ap. J.*, **172**, 639.
———. 1974, *Pub. A.S.P.*, **86**, 129.
Eggen, O. J., and Sandage, A. 1964, *Ap. J.*, **140**, 130.
Fusi Pecci, F., and Renzini, A. 1975, *Astr. Ap.*, **39**, 413.
———. 1976, *Astr. Ap.*, **46**, 447.
Harris, W. E., Racine, R., and De Roux, J. 1976, *Ap. J. Suppl.*, **31**, 13.
Hawarden, T. G. 1975, *M.N.R.A.S.*, **173**, 801.
———. 1976, *M.N.R.A.S.*, **174**, 471.
———. 1978, *M.N.R.A.S.*, **182**, 31P.
Hesser, J. E., Hartwick, F. D. A., and McClure, R. D. 1977, *Ap. J. Suppl.*, **33**, 471.
Hoffleit, D. 1964, *Catalogue of Bright Stars* (New Haven: Yale University Observatory).
Iben, I., and Rood, R. T. 1970, *Ap. J.*, **161**, 587.
Johnson, H. L. 1966, *Ann. Rev. Astr. Ap.*, **4**, 193.
Kraft, R. P., Preston, G. N., and Wolff, S. C. 1964, *Ap. J.*, **140**, 235.
Kukarkin, B. V. 1974, *The Globular Star Clusters* (Moscow: Nauka).
Lee, S. W. 1977*a*, *Astr. Ap. Suppl.*, **27**, 367.
———. 1977*b*, *Astr. Ap. Suppl.*, **27**, 381.
———. 1977*c*, *Astr. Ap. Suppl.*, **28**, 409.
Lloyd Evans, T. 1975, *M.N.R.A.S.*, **171**, 647.
Lo Presto, J. C. 1971, *Pub. A.S.P.*, **83**, 674.
Mallia, E. A. 1977, *Astr. Ap.*, **60**, 195.
Mallia, E. A., and Pagel, B. E. 1978, *M.N.R.A.S.*, **184**, 55P.
McClure, R. D., and Norris, J. E. 1974, *Ap. J.*, **193**, 139.
Menzies, J. W. 1967, Ph.D. thesis, Australian National University.
Norris, J. E., and Hawarden, T. G. 1978, *Ap. J.*, **223**, 483.
Norris, J. E., Freeman, K. C., and Seitzer, P. 1983, to be published.
Osterbrock, D. E. 1974, *Astrophysics of Gaseous Nebulae* (San Francisco: W. H. Freeman), p. 16.
Persson, S. E., Frogel, J. A., Cohen, J. G., Aaronson, M., and Matthews, K. 1980, *Ap. J.*, **235**, 452.
Peterson, R. C. 1981, *Ap. J.* (*Letters*), **248**, L31.
———. 1982, *Ap. J.*, **258**, 499.
Ramsey, L. W. 1979, *Pub. A.S.P.*, **91**, 252.
Reimers, D. 1975, in *Problems of Stellar Atmospheres and Envelopes*, ed. B. Baschek, W. H. Kegel, and G. Traving (New York: Springer), p. 229.
———. 1977, *Astr. Ap.*, **57**, 395.
Renzini, A. 1977, in *Advanced Stages in Stellar Evolution*, ed. P. Bouvier and A. Maeder, *Advanced Course of the Swiss Society of Astronomy and Astrophysics, Saas-Fee* (Geneva: Geneva Observatory), p. 149.
Rood, R. T. 1973, *Ap. J.*, **184**, 815.
Sandage, A. 1970, *Ap. J.*, **162**, 841.
Sweigart, A. V., and Gross, P. G. 1978, *Ap. J. Suppl.*, **36**, 405.
Woolley, R. 1966, *Royal Obs. Ann.*, No. 2.
Woolley, R., Alexander, J. B., Mather, L., and Epps, E. 1961, *Royal Obs. Bull.*, No. 43.
Zinn, R. 1980, *Ap. J. Suppl.*, **42**, 19.

C. CACCIARI: ESA Satellite Tracking Station, P.O. Box 54065, Madrid, Spain

K. C. FREEMAN: Mount Stromlo and Siding Spring Observatories, Private Bag, Woden P.O., A.C.T. 2606, Australia